AGU100 ADVANCING EARTH AND SPACE SCIENCE

JGR

Journal of Geophysical Research: Atmospheres

RESEARCH ARTICLE

10.1029/2017JD027771

A Terrestrial Gamma-Ray Flash inside the Eyewall of Hurricane Patricia

G. S. Bowers[1], D. M. Smith[1], N. A. Kelley[2], G. F. Martinez-McKinney[1], S. A. Cummer[3], J. R. Dwyer[4], S. Heckman[5], R. H. Holzworth[6], F. Marks[7], P. Reasor[7], J. Gamache[7], J. Dunion[7], T. Richards[8], and H. K. Rassoul[9]

[1]Santa Cruz Institute for Particle Physics and Physics Department, University of California, Santa Cruz, CA, USA, [2]Swift Navigation, San Francisco, CA, USA, [3]Department of Electrical and Computer Engineering, Duke University, Durham, NC, USA, [4]Department of Physics and Space Sciences Center (EOS), University of New Hampshire, Durham, NH, USA, [5]Earth Networks, Germantown, MD, USA, [6]Earth and Space Sciences, University of Washington, Seattle, WA, USA, [7]Hurricane Research Division, Atlantic Oceanographic and Meteorological Laboratory, NOAA, Miami, FL, USA, [8]Hurricane Hunters, Aircraft Operations Center, NOAA, Tampa, FL, USA, [9]Department of Physics and Space Sciences, Florida Institute of Technology, Melbourne, FL, USA

Key Points:
- We report the first in situ observation of a terrestrial gamma-ray flash inside a hurricane eyewall
- Observed gamma-ray spectra, lightning data, and meteorological scenario are consistent with production of a downward beam of positrons
- Simulations of the downward positron beam establish ordinary TGFs as detectable at almost any altitude

Correspondence to:
G. S. Bowers,
gsbowers@ucsc.edu;
gsbowers@lanl.gov

Citation:
Bowers, G. S., Smith, D. M., Kelley, N. A., Martinez-McKinney, G. F., Cummer, S. A., Dwyer, J. R., et al. (2018). A terrestrial gamma-ray flash inside the eyewall of Hurricane Patricia. *Journal of Geophysical Research: Atmospheres*, *123*, 4977–4987. https://doi.org/10.1029/2017JD027771

Received 22 SEP 2017
Accepted 24 APR 2018
Accepted article online 4 MAY 2018
Published online 17 MAY 2018

Abstract On 23 October 2015 at ~1732 UTC, the Airborne Detector for Energetic Lightning Emissions (ADELE) flew through the eyewall of Hurricane Patricia aboard National Oceanic and Atmospheric Administration's Hurricane Hunter WP-3D Orion, observing the first terrestrial gamma-ray flash (TGF) ever seen in that context, and the first ever viewed from behind the forward direction of the main TGF gamma-ray burst. ADELE measured 184 counts of ionizing radiation within 150 μs, coincident with the detection of a nearby lightning flash. Lightning characteristics inferred from the associated radio signal and comparison of the gamma-ray energy spectrum to simulations suggests that this is the first observation of a reverse beam of positrons predicted by the leading TGF production model, relativistic runaway electron avalanches. This paper presents the first experimental evidence of a previously predicted second component of gamma-ray emission from TGFs. The brightest emission, commonly observed from orbit, is from the relativistic runaway electron avalanche bremsstrahlung; the second, fainter component reported here is from the bremsstrahlung of positrons propagating in the reverse direction. This reverse gamma-ray beam penetrates to low enough altitudes to allow ground-based detection of typical upward TGFs from mountain observatories.

Plain Language Summary We report the first observation of gamma-ray emission from lightning within a hurricane eyewall, consistent with production by a downward beam of positrons.

1. Introduction

Terrestrial gamma-ray flashes (TGFs) are avalanches of relativistic electrons created in thunderstorm electric fields that scatter off molecules in the Earth's atmosphere and produce intense, submillisecond beams of X-ray and gamma ray emissions routinely observed by detectors aboard satellites (Briggs et al., 2010; Fishman et al., 1994; Marisaldi et al., 2010; Smith et al., 2005; Ursi et al., 2017), and occasionally from detectors in the air (D. M. Smith et al., 2011), and on the ground (Abbasi et al., 2017; Bowers et al., 2017; Enoto et al., 2017; Hare et al., 2016; Tran et al., 2015). Most TGFs are associated with positive intracloud (+IC) lightning (Cummer et al., 2005; Stanley et al., 2006), and their observed energy spectra and radio emissions are consistent with relativistic runaway electron avalanche (RREA) production at altitudes of 10–14 km (Cummer et al., 2015; Dwyer et al., 2012; Dwyer & Smith, 2005; Dwyer & Uman, 2014; Shao et al., 2010). It is estimated that worldwide ~1,000 TGFs capable of being observed by satellite occur per day (Briggs et al., 2013). Although TGFs seem to occur in a small fraction of lightning (Smith et al., 2016), the radiation dose received from flying through a TGF beam aboard a passenger jet can present a significant hazard to both individuals (Dwyer et al., 2010) and avionics (Tavani et al., 2013) and is a motivation for the continued study of these high-energy atmospheric phenomena.

We constructed a gamma-ray instrument to be deployed on aircraft to observe radiation from lightning. The goal of these observations was to measure the brightness and energy spectra of nearby TGFs to compare to models and satellite data. TGFs observed by satellites are consistent with simulations of an RREA process

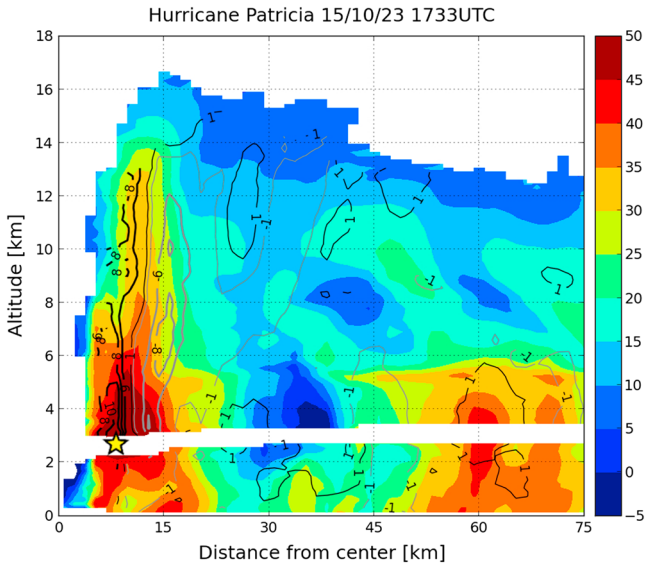

Figure 1. Vertical cross section of radar reflectivity (dBZ) measured by the X-band tail radar of NOAA's WP-3D Orion during its first inbound pass through Hurricane Patricia's eyewall on 23 October 2015 at ~1730 UTC. The yellow star indicates ADELE's location during the TGF observation at 17:32:06 UTC at an altitude of 2.6 km, ~7.5 km away from the hurricane center at 18.167°N, 105.267°W; ±1, 6, 8, and 10 m/s contours of the vertical component of the wind velocity are shown in black/grey.

producing 10^{16}–10^{19} gamma rays (Cummer et al., 2005; Dwyer et al., 2017; Mailyan et al., 2016). Airborne observations provide an opportunity to discover if there exist TGFs too faint or low in the atmosphere to be seen by satellites, as well as a means to observe TGFs from angles and positions impossible from space.

2. Airborne Detector for Energetic Lightning Emissions Mark II

The Airborne Detector for Energetic Lightning Emissions (ADELE) mark II measures X-rays and gamma rays aboard aircraft flown into or above thunderstorm systems, to observe TGFs up close, and is more compact than the original instrument (Smith et al., 2011). In 2014 and 2015 ADELE mark II flew aboard National Oceanic and Atmospheric Administration (NOAA)'s WP-3D Orion during the Atlantic hurricane season, targeting thunderstorm systems in hurricane rainbands (Cecil et al., 2002), and the increased eyewall lightning associated with the intensification of strong hurricanes (Price et al., 2009).

The ADELE mark II instrument consists of three scintillation detectors. The detectors are scintillators encapsulated with and mounted to a photomultiplier tube inside a Mu-metal shielded housing. The three scintillators are a 1 × 1″ (diameter × height) small plastic scintillator, a 5 × 5″ large plastic scintillator, and a 3 × 3″ lanthanum bromide $LaBr_3$(Ce) crystal.

The plastic detector photomultiplier tubes (Electron Tubes models 9272B and 9275B with custom transistorized bases, for the 1 × 1″ and 5 × 5″ detectors, respectively) are powered by an EMCO CA12N-5 High Voltage Power Supply that can source up to 0.8 mA at 1,250 V and require 5VDC to operate, provided by an Acopian Gold Box Linear Regulated AC-DC power supply V5GT200D-5GT200DM. The $LaBr_3$(Ce) detector is powered using an Ortec 296 ScinitiPack Photomultiplier Base.

Each detector is connected to one or more custom discriminator boards that split the input into four channels that are converted to a low-voltage differential-signal (LVDS) output. Each channel is initially passed through a clamping amplifier and inverter. The two channels corresponding to the lowest threshold undergo an additional stage of 10X amplification. Each channel is input into a discriminator circuit that converts the pulse into a 5 V "time-above-threshold" LVDS signal. For each detector, one discriminator threshold was calibrated directly using a known energy deposit from a ^{137}CS radioactive source—the photopeak at 662 keV for the $LaBr_3$ detector, and the Compton shoulder below 478 keV for the plastic detectors. The linearity of the electronics having been demonstrated using a pulser, and the approximate linearity of the light output of the scintillators being well known, the remaining thresholds were set using tunable resistors to be desired multiples of the calibrated channel. The calibration was verified using an additional source (^{152}Eu, with multiple lines up to 1.4 MeV), and Monte Carlo simulations using GEANT4 of the expected relative count rates among the channels.

The LVDS threshold signals are sent over twisted pair in a shielded Ethernet cable to a Virtex 6 ML605 development board FPGA where the LVDS signal is digitized at 200 MHz (5 ns sampling intervals), and the number of counts and deadtime counts per 50 μs is calculated. A count is any transition from the LVDS low state (0 V) to the LVDS high state (5 V). A deadtime count is a 5 ns tick when the LVDS signal is in the high state. The total number of sampling intervals within a 50 μs time bin is 10,000, and the fractional deadtime is the number of deadtime counts divided by this number. The counts and deadtime counts per 50 μs interval are recorded into 1 s packets and sent over Ethernet to a single board computer where the data packets are written to external solid state drives.

The FPGA clock is conditioned by the pulse per second from a Garmin 15xH GPS OEM module and has an absolute timing accuracy of 50 μs.

The lowest channel of the $LaBr_3$ detector (>100 keV) was unusable due to noise, and the upper two channels (>10 MeV, >15 MeV) were not usable after discovering that the ScintiPack photomultiplier base clips output pulses above a threshold voltage corresponding to ~6 MeV.

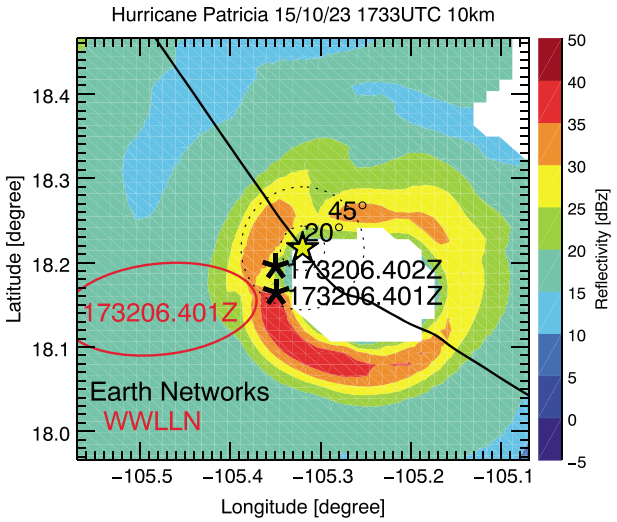

Figure 2. Horizontal cross section of radar reflectivity at 10 km inside Hurricane Patricia showing eyewall structure and reported lightning locations during the TGF observation. The yellow star indicates the location of ADELE at 17:32:06.401UTC. The red ellipse shows the RMS location uncertainty for a flash recorded by the World Wide Lightning Location Network (WWLLN) at 17:32:06.401UTC. The black asterisks show locations of two flashes located by Earth Networks at 17:32:06.401 and 17:32:06.402UTC, with location uncertainties comparable to the ellipse shown for WWLLN. The dashed circles show the footprint at the plane's altitude of 2.6 km from downward beams originating at 10 km with opening half angles of 20 and 45°.

3. A TGF in the Eyewall of Hurricane Patricia

On 23 October, ~1733 UTC, NOAA's Hurricane Hunters' WP-3D flew through the center of Hurricane Patricia during meteorological reconnaissance (Figure 1). At 1732 UTC, at an altitude of ~2.6 km (Figure 2), within 100 μs of a nearby lightning flash (Figure 3), ADELE measured 184 counts of ionizing radiation within 150 μs among its three scintillation detectors (Figure 4 and Table 1).

At this time, Patricia had briefly become "the strongest hurricane on record in either the eastern North Pacific or North Atlantic Basins" (Rogers et al., 2015). This WP-3D pass through the eyewall occurred approximately 3.5 hr after peak intensity, in the middle of a 4-hr interval of intense lightning observed by the Worldwide Lightning Location Network (WWLLN); an even more intense interval of lightning had occurred up to 1000 UTC, during the period of most rapid intensification. This is the first reported observation of a TGF associated with a hurricane eyewall, although TGFs have been seen from a very wide range of storm types (Chronis et al., 2016; Splitt et al., 2010). All previously observed TGFs associated with tropical storms have been observed in the rainbands, predominately during the strengthening phase of the storm (Roberts et al., 2016)

The characteristics of the radio signal from the nearby lightning flash (Figure 5) indicate that this was a typical TGF, consistent with the current interpretation of a beam of RREA electrons moving upward. The ratio of the azimuthal and radial components of the measured magnetic field was found to be consistent with the WWLLN and Earth Networks Total Lightning Network identified signals in the hurricane eyewall. The polarity of the radio signal is consistent with both +IC (intracloud) and +CG (cloud to ground) discharge processes, but a few waveform characteristics suggest that +IC is more likely. One is the fairly low charge moment change of 22 C km, which is three times smaller than the high peak current −CG that comes later, and −CG flashes on average have lower charge moment changes than +CGs (Williams et al., 2007). Additionally, the presence of two discrete pulses separated by about a millisecond that appear to come from the same location is uncommon for +CGs but quite common for +ICs associated with TGFs, indicating an ascending leader (Cummer et al., 2015).

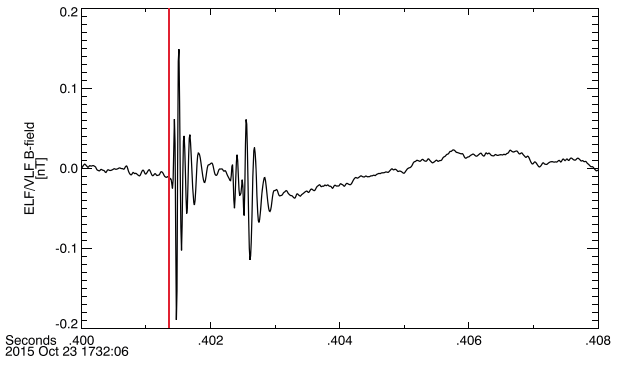

Figure 3. Associated radio waveform recorded by a very low frequency sensor at Duke University. The time of the radio signal is shown for an observation made at the aircraft. This is inferred from the observed signal time at the Duke very low frequency sensor minus 10.82 ms corresponding to the speed of light propagation time over a propagation distance of 3,242.5 km, corresponding to the WGS-84 distance from the aircraft to the Duke sensor. The red vertical bar shows the time of the TGF observation at the aircraft. The TGF observation being within 100 μs of the start of the radio signal is consistent with the definition of "simultaneity" from (Connaughton et al., 2013).

The plastic scintillator and $LaBr_3$ pulse widths are on the order of 100 and 250 ns, respectively. To calculate the deadtime-corrected count rate in each detector channel (Table 1), we use the paralyzable model for deadtime correction (Knoll, 2010). To produce a piled-up count in a given channel, two counts that would trigger the channel immediately below must occur at the same time (since the spacing between channels is on the order of a factor of 2). To estimate the number of piled-up counts in a given detector channel, we multiply the deadtime fraction of the next lowest detector channel (the ratio of deadtime counts to the total number of possible counts per 50 μs interval) by the count rate in the same (next lowest) detector channel. This gives a conservative estimate of the number of counts within a detector channel due to pileup per 50 μs interval and is <1 for the most active channel during the TGF.

In addition to an upward avalanche of electrons, RREA theory also predicts a beam of positrons moving downward, produced by the interaction of gamma rays with atomic nuclei (Dwyer, 2003, 2012). Both electron and positron beams are expected to produce bremsstrahlung X-rays and gamma rays in their direction of travel by colliding with atomic nuclei (Figure 6), but only the bright upward gamma-ray beam produced by the electrons has ever been observed from a TGF. In the feedback model

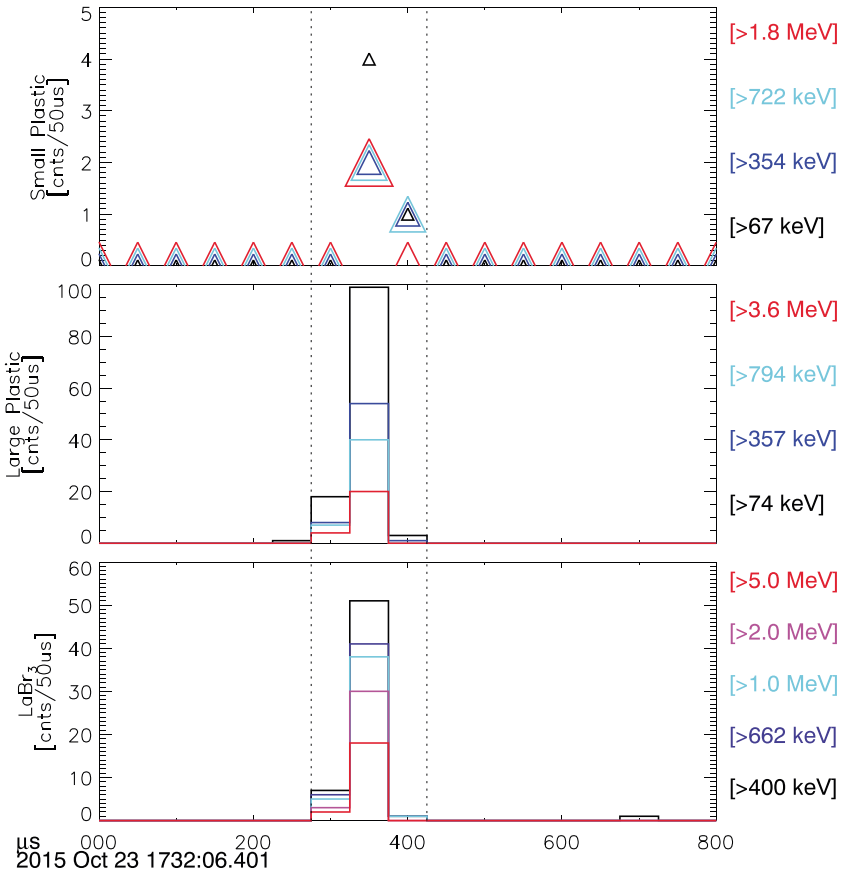

Figure 4. Raw count rate data of the Hurricane Patricia TGF observed by ADELE showing scintillation counts per 50 μs in ADELE's 15 integral energy channels: (top) 1 × 1″ plastic scintillator, (middle) 5 × 5″ plastic scintillator, and (bottom) 3 × 3″ lanthanum bromide ($LaBr_3$) scintillator. About 184 unique counts were observed within the 150 μs indicated by the vertical dashed lines.

Table 1
Raw Count and Deadtime Count for Each ADELE Detector's Energy Channel Recorded Over 150 μs Duration of TGF

Channel	17:32:06.40130		17:32:06.40135		17:32:06.40140		Total	
	Counts	Deadtime counts	Counts	Deadtime counts	Counts	Deadtime counts	Counts	Deadtime counts
SmPl								
>67 keV	0	0	4	33	1	8	5	41
>354 keV	0	0	2	13	1	4	3	17
>722 keV	0	0	2	10	1	2	3	12
>1,800 keV	0	0	2	5	0	0	2	5
LgPl								
>74 keV	18	289	99	1,890	3	24	120	2,203
>357 keV	8	100	54	639	1	4	63	743
>794 keV	7	85	40	488	0	0	47	573
>3,586 keV	4	23	20	120	0	0	24	143
$LaBr_3$								
>415 keV	7	133	51	1,187	1	13	59	1,333
>662 keV	6	80	41	599	1	10	48	689
>1,060 keV	5	61	38	515	1	5	44	581
>1,980 keV	3	46	30	553	0	0	33	599
>4,980 keV	2	16	18	210	0	0	20	226

Note. The timestamps correspond to the beginning of the 50 μs time bin.

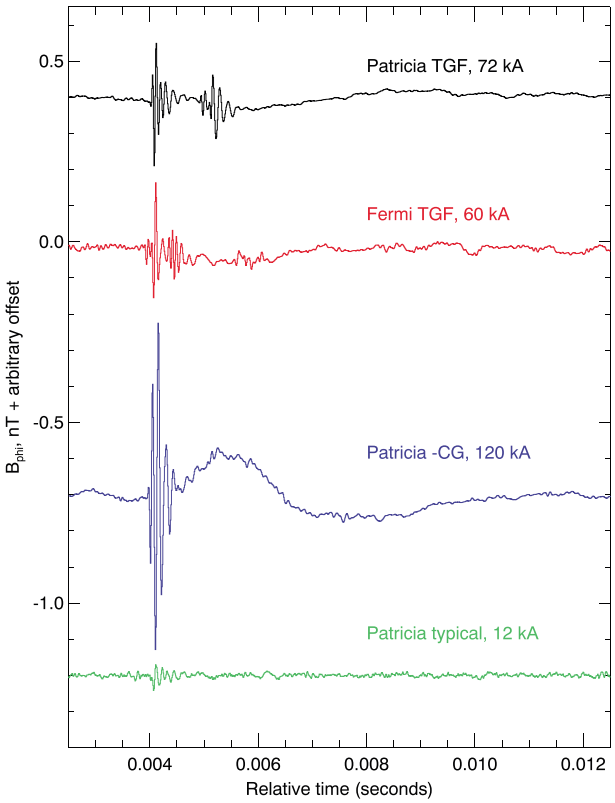

Figure 5. Comparison of radio signal waveforms from lightning flashes detected by the Duke very low frequency sensor. Lightning characteristics are inferred from the fast (~5 periods in 500 μs) and slow (trailing pulse with ~2 ms duration) signals in the waveform. The leading sign of the slow signal unambiguously identifies the polarity of the event: A negative leading slow signal indicates a negative charge moving upwards. Two fast signals in rapid succession are very typical of an intracloud lightning event. (top, black) Radio signal from the lightning flash coincident with the hurricane Patricia TGF observation. (red) Radio signal from a lightning flash coincident with a Fermi satellite TGF observation, located at a comparable distance to the Duke sensor as Hurricane Patricia. (blue) Radio signal from a −CG lightning flash observed in Hurricane Patricia. (green) Radio signal from typical lightning flash in Hurricane Patricia. The currents listed above each flash are NLDN-equivalent peak current estimates, derived from Duke very low frequency data with a standard error of 30% as described in (Lu et al., 2011).

of TGFs (Dwyer, 2008), it is the downward positron beam that is responsible for the enormous brightening of TGFs by seeding new electron avalanches at the bottom of the avalanche region, but the reverse positron beam is an intrinsic part of every RREA avalanche regardless of whether feedback is significant —it relies only on the unavoidable process of pair production by gamma rays inside the avalanche region, and can be absent only if the region is extremely small Upward positron beams have been observed from lightning discharges (Briggs et al., 2011), but these are a by-product of the TGF photon interactions in the outer layers of Earth's atmosphere above the thunderstorm, whereas the downward positron beam is a direct product of the interactions in the TGF's high-electric-field production region.

4. Monte Carlo Simulations of TGF Positron Interactions

To compare our observations to a typical TGF seen from satellite, assuming an RREA production mechanism, the energy spectra of counts recorded within the 150 μs were compared to Monte Carlo simulations using GEANT4 (Agostinelli et al., 2003; Allison et al., 2006, 2016) of ADELE's response to the downward beam of positron bremsstrahlung produced from an upward TGF occurring at altitudes 8, 10, and 12 km. In each simulation, several billion gamma rays with the energy and angular distribution expected from an RREA TGF positron beam (Figure 7) were released at the specified altitude and allowed to propagate through and interact with a mass model of the atmosphere, and the resulting radiation field produced at the planes altitude of 2.6 km was captured. The input distributions (Figure 7) come from simulations of TGFs using the Reletivstic Electron Avalanche Model (REAM) discussed in Dwyer (2003, 2007). The energy distribution for the positron bremsstrahlung is closely approximated by the functional form (red dotted line) $f(E) \sim \exp(-E_0/(E_0^{0.85} - E^{0.85}))/E$, where $E_0 = 100$ MeV. The energy distribution for the full avalanche model is closely approximated by the functional form (black dotted line) $f(E) \sim \exp(-E/6.3\ \text{MeV})/E$. The ratio of upward gammas from the full avalanche to downward gammas from positron bremmstrahlung is ~180. The solid angle distribution follows the intrinsic beam shape from the REAM simulations, and for the positron bremmstrahlung is beamed narrowly downward (toward 180°). This simulation assumed an electric field strength of 400,000 kV/m (sea level equivalent).

For each simulated RREA source altitude, a mass model of ADELE in the NOAA aircraft was positioned at several radial distances from the nadir of the downward positron beam at 0 degrees. The radiation field captured from the first stage of the simulation was then allowed to scatter and be absorbed in the instrument and aircraft. The shape of the simulated spectra in all three detectors closely resembles the observed spectra (Figure 8).

5. TGF Spectra Comparison (Downward e+, Upward e−, and Upward e− Backscatter)

To test the hypothesis that our observation was from the bremsstrahlung of the downward positron beam of an upward TGF, and not from another TGF source or orientation, we considered a tripole charge structure with a main negative region extending from 5 to 8 km, with lower and upper positive regions at 5 and 8 km, respectively. In this scenario it is plausible for either an upward TGF to occur near 8 km associated with a +IC discharge, or a downward TGF to occur near 5 km associated with a −IC discharge. It is also possible, if the tripole charge structures were inverted, that an upward TGF could occur near 5 km associated with a +IC between the lower negative and main positive. We compared the shape of the gamma-ray spectrum

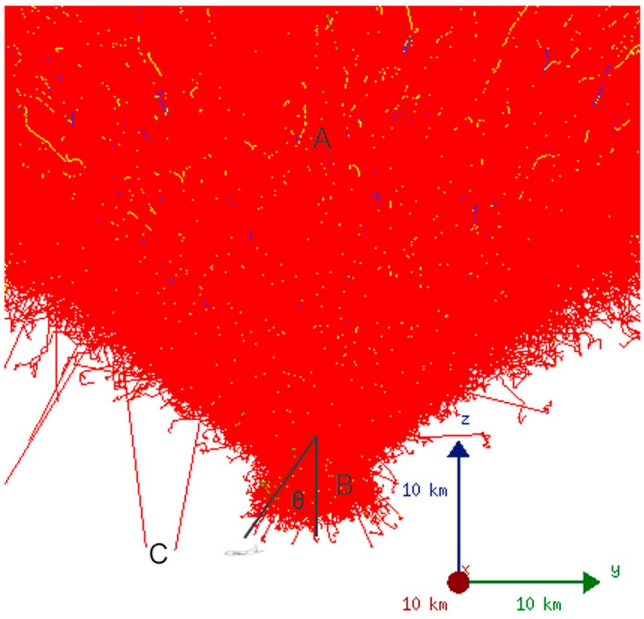

Figure 6. Monte Carlo simulation of an upward TGF in Earth's atmosphere at 10.5 km showing gamma-ray bremsstrahlung emissions (red) from upward electrons (A), downward positrons (B), and backscattered gamma rays originally from upward-moving electrons (C). The yellow/blue tracks are secondary electrons/positrons. Plane shown at an observation angle θ.

produced at 2.6 km from (a) the bremsstrahlung from the downward electron beam of a reverse TGF at 5 km, (b) the electron backscatter from an upward TGF at 4 km (the highest altitude that produced significant counts in our simulated detector), with no reverse positron beam, and (c) the bremsstrahlung from a reverse positron beam generated by an upward TGF as predicted by RREA at 8 km (Figure 9).

The spectral shape from a reverse positron beam is seen to be harder (more counts at higher energies) than that from the direct electron beam, but the spectra are similar enough that with the number of counts we observed, without lightning polarity information from the radio observation (Figures 3 and 5), we would likely not distinguish the two cases. We rely on the radio polarity primarily, and the implied need for an unusual charge structure secondarily, to rule out a downward TGF.

For the tripole charge structure considered, the electron backscatter from an upward TGF at 8 km (with no downward positron beam) is undetectable. At 4 km (an unrealistic source altitude for this model), the electron backscatter from an upward TGF (with no downward positron beam) could not reproduce the observed energy spectra, the backscattered spectra being much softer than what was observed (see Figure 9).

6. TGF Source Altitude: Meteorological Evidence

The simulated spectra (Figure 7) are similar for the source altitudes considered and all energies below 10 MeV. This is due to a balance between the increasing loss of low energy gamma rays due to absorption and the increasing production of low energy gamma rays from the downscattering of high-energy gammas to lower energies as the amount of atmosphere between the instrument and the TGF increases. The simulated spectra begins to differ for energies above 10 MeV for different altitudes and angles, as seen in the >5 MeV channel for $LaBr_3$, but not enough to constrain the likely TGF source altitude based on the statistical uncertainties of these measurements (Gehrels, 1986).

Detailed meteorological observations of a storm system that produced a TGF observed by satellite in 2008 found the associated +IC leader occurred at an altitude corresponding to a region of radar reflectivity between

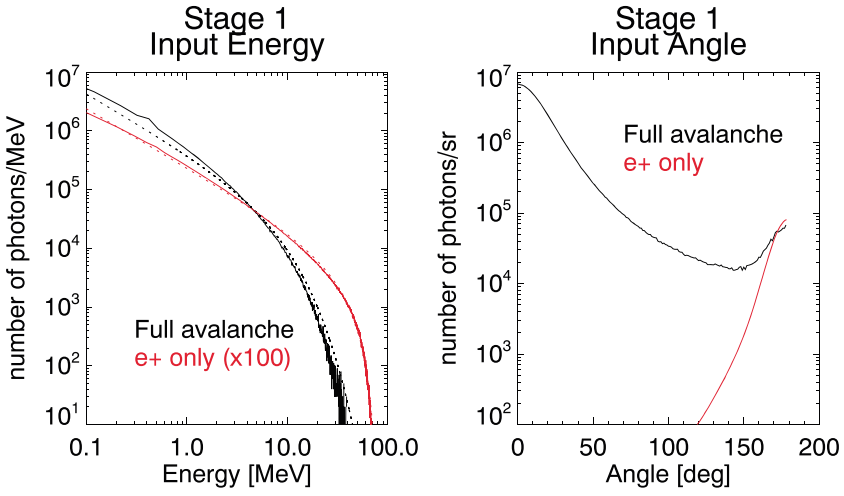

Figure 7. (left) Energy and (right) angular distribution of gamma rays produced by the bremsstrahlung of a full TGF RREA avalanche (black) and the downward positrons only (red). The dotted lines show the functional forms for energy distributions provided in text.

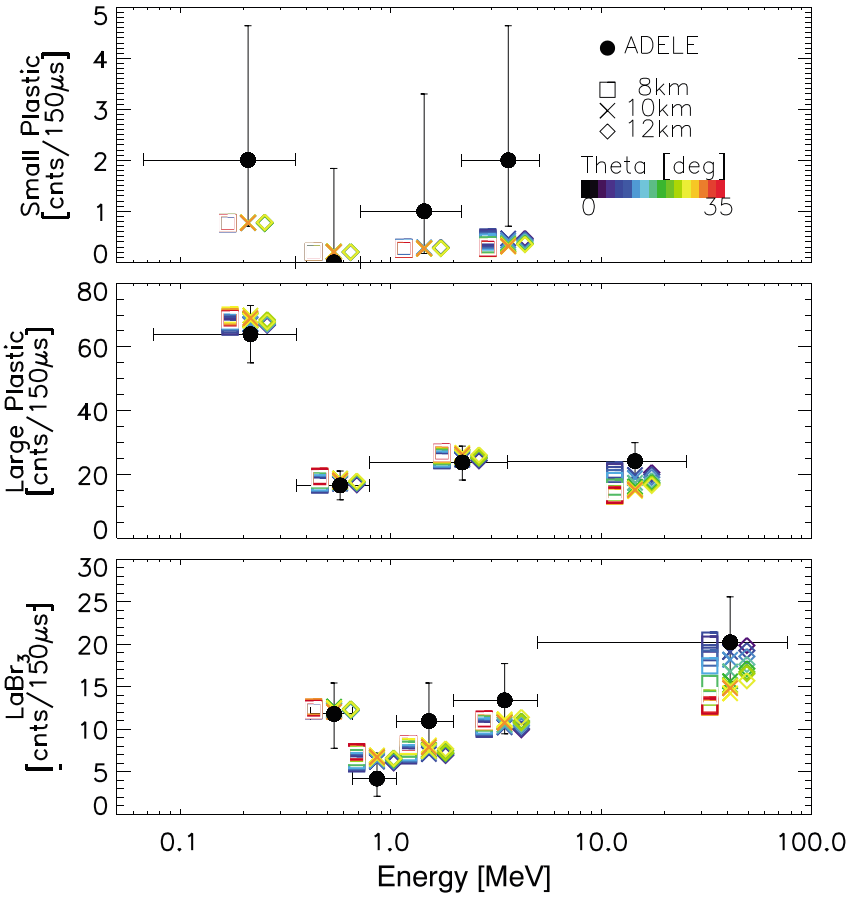

Figure 8. Number of deadtime corrected scintillator counts observed by ADELE (black circles) in each detector. The colored symbols (square, cross, and diamond) for comparison are simulated counts from a Monte Carlo simulation of ADELE at an altitude of 2.6 km, below the downward positron beam of an upward pointing TGF at an altitude of 8, 10, and 12 km. The colors indicate the angular offset of ADELE at 2.6 km with respect to the nadir of the positron beam. The vertical bars on the observed counts are the 84% confidence limits in the observed counts (Gehrels, 1986). The horizontal bars correspond to the widths of the energy channels in the detectors.

20 and 25 dBZ (Lu et al., 2010). From the vertical radar reflectivity measurements (Figure 1), this range of reflectivity corresponds to a range of altitudes between 8 and 10 km. However, it should be noted that the TGF likely occurred out of the plane of the vertical measurement where the reflectivity profile may have been different.

In situ observations of electrical activity in hurricane eyewalls indicate that the supercooled cloud water content necessary for electrification increases for vertical velocities $\gtrsim$5.0 m/s (Black & Hallett, 1999), indicating that lightning discharges during our observation were most likely in the eyewall tower above the aircraft (Figure 1).

TGFs have predominately been observed to occur coincident with +IC lightning, as an upward negative leader from the main negative charge region approaches the upper positive region. The boundary between the upper positive and main negative, where the TGF source region is likely to occur, is associated with the altitude where the temperature equals the so-called "charge reversal temperature," between −20 and −10 °C (Saunders & Peck, 1998; Takahashi, 1978). This isotherm can therefore serve as a meteorological indicator of a likely TGF source region. Temperature versus altitude profiles from dropsonde data taken during the Tropical Cyclone Intensity (TCI) experiment (Bell et al., 2016) inside Hurricane Patricia on 23 October at 2000UTC are shown in Figure 10. The charge reversal temperature inside the eyewall is shown to occur between 8 and 10 km. Although we cannot say anything definitive about the temperature profile during the TGF observation at 1736UTC, because the temperature profile is seen to be warmer in the inner eyewall compared to the outer rainbands, it is plausible that the temperature profile earlier would have been similar or warmer, leading to a comparable or higher altitude for the charge reversal temperature region.

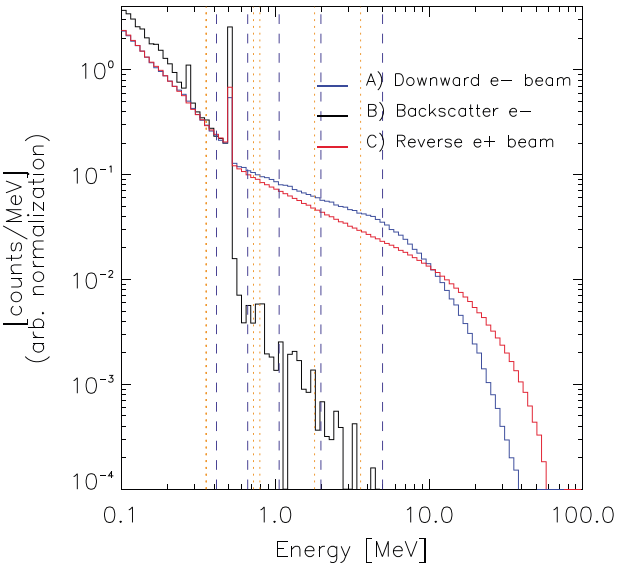

Figure 9. The spectra at 2.6 km produced by (A) the direct electron (e−) beam from a downward TGF at 5 km, (B) the electron backscatter from an upward TGF at 4 km (with no positron beam), and (C) the reverse positron (e+) beam from an upward TGF at 8 km. ADELE's integral energy channel thresholds are shown by the vertical dashed lines (plastic detectors, find-dashed orange; $LaBr_3$, dashed blue).

7. Conclusions

From our observations and the simulated response of ADELE in the downward positron beam of a TGF, we can infer the total number of gamma rays >1 MeV produced by the TGF for a given range of source altitudes and observation angles and compare to the range of total gamma rays >1 MeV produced by TGFs that have been observed by satellites (Mailyan et al., 2016; Figure 11). Mailyan's paper reports TGF brightness in terms of the total number of electrons >1 MeV produced by each TGF, which we convert to equivalent total number to gamma rays >1 MeV using the ratio 0.29 TGF gammas (> 1 MeV) per TGF electron (>1 MeV) based on results from the REAM simulation code (Dwyer, 2007).

For angles relatively far from the nadir (which are more likely both by pure geometry and placement of the high-reflectivity parts of the eyewall in Figure 2), the total number of inferred gamma-rays is consistent with ordinary TGFs seen from space, just as the current moment of the slow component of the sferic was (Figure 5). Although we cannot constrain the TGF source altitude from the radio measurements or observed gamma-ray spectra (see section 5), it is plausible, from comparing high-resolution simulations of the charge structure evolution of electrically active hurricanes (Fierro et al., 2015) to previously observed charge structures of TGF source regions, that the TGF occurred between 8 and 12 km, which is also consistent with simultaneous radar measurements of the cloud reflectivity during the observation, and later dropsonde measurements of the eyewall temperature profile at 2000 UTC (see section 6). A source region below 8 km, but above the airplane, would indicate a TGF too dim to be observed by satellite.

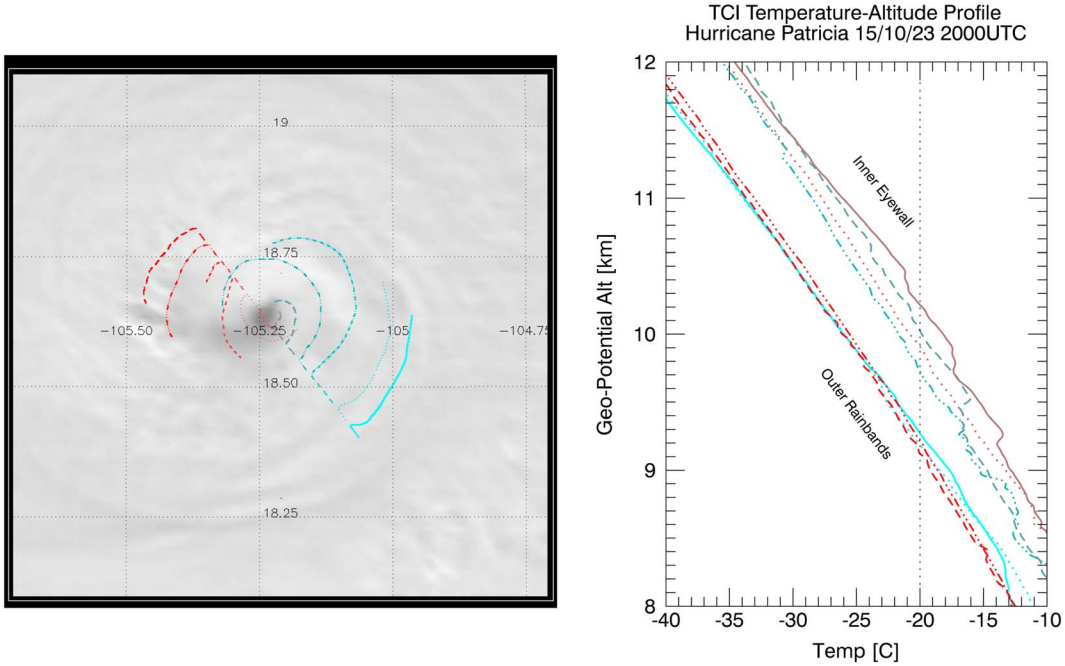

Figure 10. (left) Path of dropsondes in Hurricane Patricia during the TCI experiment on 23 October 2015 at 2000 UTC, overplotted on GOES13 14.7 μm image data taken at 194519 UTC (image data shifted 0.83° in longitude to compensate for viewing parallax). (right) Temperature profiles versus altitude from dropsonde data. The −20 °C charge reversal temperature is indicated by the vertical dotted line. The data and trajectory for an individual dropsonde are identified by the combination of a unique line color and style.

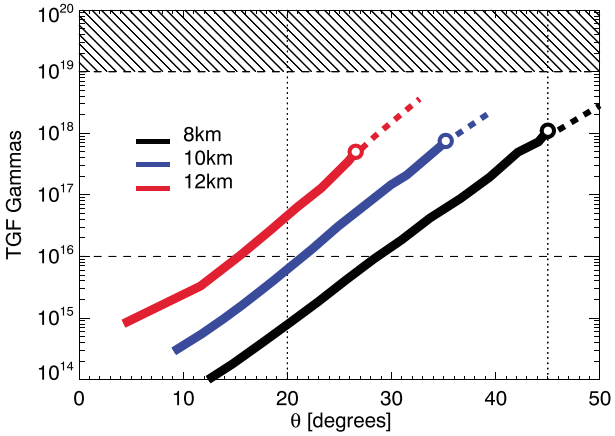

Figure 11. Estimated brightness of an upward TGF in number of gammas >1 MeV for likely TGF altitudes determined by the observation angle of the aircraft relative to the nadir of the TGFs downward positron beam. Between 10^{16} and 10^{19} gammas (dashed horizontal lines) is the typical range of TGF brightness observed by satellites (Mailyan et al., 2016). A brightness above 10^{19} gammas per TGF is excluded based on existing satellite observations. A brightness below 10^{16} gammas per TGF is possible but is too dim to likely be observed by satellite. The region marked by vertical lines at 20 and 45° corresponds to the footprint shown in Figure 2. For a given altitude, the white circles correspond to a TGF brightness assuming that the 72 kA peak current measured by Earth Networks was entirely from the radio emissions of the TGF electrons (Dwyer & Cummer, 2013; meaning no current flowed in the lightning channel) and represents an upper limit on the TGF brightness based on current RREA models (dashed segments are therefore unphysical).

The simulated spectra from a downward TGF above the airplane (requiring a −IC discharge) is also consistent with our observations but is ruled out based on the radio polarity. The simulated spectrum from the backscatter of an upward TGF without a downward beam of positrons (Figure 9c) is found to be too soft and cannot reproduce the observed counts at high energies (see section 5). We therefore conclude that the most likely scenario is that the TGF reverse positron beam, never before observed but predicted by RREA theory, is indeed present.

One implication of this observation and the simulations we preformed is that the upward TGFs often seen from space may be much more easily observable from the ground, particularly from high altitudes, than has previously been assumed. We establish relatively normal TGFs as events that can pierce Earth's atmosphere almost from top to bottom. There was no shortage of counts in this event, which was probably a typical upward TGF, and mountaintops higher than the 2.6 km altitude of the aircraft during this event are not uncommon. In fact, using the attenuation formula for RREA gamma rays from D. M. Smith et al. (2010) of 45 g/cm^2 for each *e*-folding in number of counts, our 184-count TGF at 2.6 km would have given 20 counts, still easily detectable above background, at a 1.6 km mountain station. Because the positron bremsstrahlung gamma rays are higher in energy and more penetrating than the electron bremsstrahlung spectrum considered in that work, this is in fact an underestimate. The primary obstacle to frequent observations of this type is the much smaller footprint of the TGF beam on the ground compared to its footprint in low Earth orbit.

This paper presents clear evidence that TGFs can be observed in two ways: one, where the observation is made in front of the forward direction of the RREA bremsstrahlung, as is likely the case for all satellite observations made to date (Briggs et al., 2010; Fishman et al., 1994; Marisaldi et al., 2010; Smith et al., 2005; Ursi et al., 2017), and all observations seen from the ground where the forward direction of the RREA bremsstrahlung is beamed downward (Abbasi et al., 2017; Bowers et al., 2017; Enoto et al., 2017; Hare et al., 2016; Tran et al., 2015), and second, where the observation is made from behind the forward direction of the RREA bremsstrahlung, where it is possible to observe positron bremsstrahlung from the reverse positron beam created by the forward electron RREA.

Acknowledgments

The authors wish to thank the World Wide Lightning Location Network (http://wwlln.net), a collaboration among over 50 universities and institutions, for providing the lightning location data used in this paper. The authors wish to thank the TCI Department Research Initiative and the Office of Naval Research for their support. All data and software used in this study can be obtained by the corresponding author upon request. The observational data presented in this work is available to download at https://research-archive.scipp.ucsc.edu/adele/notes/151023/173206/observations. The simulated data used in this work are available to download at https://research-archive.scipp.ucsc.edu/adele/notes/151023/173206/simulations. This research was funded by NSF grants AGS-1160226, AGS-1613028, and AGS-1612466.

References

Abbasi, R. U., Abu-Zayyad T., Allen M., Azuma R., Barcikowski E., Belz J. W., et al. (2017). Gamma-ray showers observed at ground level in coincidence with downward lightning leaders, ArXiv e-prints, 1705.

Agostinelli, S., Allison, J., Amako, K., Apostolakis, J., Araujo, H., Arce, P., et al. (2003). GEANT4 - a simulation toolkit. *Nuclear Instruments and Methods in Physics Research A*, *506*(3), 250–303. https://doi.org/10.1016/S0168-9002(03)01368-8

Allison, J., Amako, K., Apostolakis, J., Araujo, H., Arce Dubois, P., Asai, M., et al. (2006). Geant4 developments and applications. *IEEE Transactions on Nuclear Science*, *53*(1), 270–278. https://doi.org/10.1109/TNS.2006.869826

Allison, J., Amako, K., Apostolakis, J., Arce, P., Asai, M., Aso, T., et al. (2016). Recent developments in GEANT4. *Nuclear Instruments and Methods in Physics Research A*, *835*, 186–225. https://doi.org/10.1016/j.nima.2016.06.125

Bell, M. M., et al. (2016). ONR Tropical Cyclone Intensity 2015 NASA WB-57 HDSS Dropsonde Data, Version 1.0. https://doi.org/10.5065/D6KW5D8M

Black, R. A., & Hallett, J. (1999). Electrification of the hurricane. *Journal of the Atmospheric Sciences*, *56*(12), 2004–2028. https://doi.org/10.1175/1520-0469(1999)056%3C2004:eoth%3E2.0.co;2

Bowers, G. S., Smith, D. M., Martinez-McKinney, G. F., Kamogawa, M., Cummer, S. A., Dwyer, J. R., et al. (2017). Gamma ray signatures of neutrons from a terrestrial gamma ray flash. *Geophysical Research Letters*, *44*, 10,063–10,070. https://doi.org/10.1002/2017GL075071

Briggs, M. S., Connaughton, V., Wilson-Hodge, C., Preece, R. D., Fishman, G. J., Kippen, R. M., et al. (2011). Electron-positron beams from terrestrial lightning observed with Fermi GBM. *Geophysical Research Letters*, *38*, L02808. https://doi.org/10.1029/2010GL046259

Briggs, M. S., Fishman, G. J., Connaughton, V., Bhat, P. N., Paciesas, W. S., Preece, R. D., et al. (2010). First results on terrestrial gamma ray flashes from the Fermi gamma-ray burst monitor. *Journal of Geophysical Research*, *115*, A07323. https://doi.org/10.1029/2009JA015242

Briggs, M. S., Xiong, S., Connaughton, V., Tierney, D., Fitzpatrick, G., Foley, S., et al. (2013). Terrestrial gamma-ray flashes in the Fermi era: Improved observations and analysis methods. *Journal of Geophysical Research: Space Physics*, *118*, 3805–3830. https://doi.org/10.1002/jgra.50205

Cecil, D. J., Zipser, E. J., & Nesbitt, S. W. (2002). Reflectivity, ice scattering, and lightning characteristics of hurricane eyewalls and rainbands. Part I: Quantitative description. *Monthly Weather Review*, *130*, 769.

Chronis, T., Briggs, M. S., Priftis, G., Connaughton, V., Brundell, J., Holzworth, R., et al. (2016). Characteristics of thunderstorms that produce terrestrial gamma ray flashes. *Bulletin of the American Meteorological Society*, *97*(4), 639–653. https://doi.org/10.1175/BAMS-D-14-00239.1

Connaughton, V., Briggs, M. S., Xiong, S., Dwyer, J. R., Hutchins, M. L., Grove, J. E., et al. (2013). Radio signals from electron beams in terrestrial gamma ray flashes. *Journal of Geophysical Research: Space Physics*, *118*, 2313–2320. https://doi.org/10.1029/2012JA018288

Cummer, S. A., Lyu, F., Briggs, M. S., Fitzpatrick, G., Roberts, O. J., & Dwyer, J. R. (2015). Lightning leader altitude progression in terrestrial gamma-ray flashes. *Geophysical Research Letters*, *42*, 7792–7798. https://doi.org/10.1002/2015GL065228

Cummer, S. A., Zhai, Y., Hu, W., Smith, D. M., Lopez, L. I., & Stanley, M. A. (2005). Measurements and implications of the relationship between lightning and terrestrial gamma ray flashes. *Geophysical Research Letters*, *32*, L08811. https://doi.org/10.1029/2005GL022778

Dwyer, J. R. (2003). A fundamental limit on electric fields in air. *Geophysical Research Letters*, *30*(20), 2055. https://doi.org/10.1029/2003GL017781

Dwyer, J. R. (2007). Relativistic breakdown in planetary atmospheres. *Physics of Plasmas*, *14*(4), 042901–042,901. https://doi.org/10.1063/1.2709652

Dwyer, J. R. (2008). Source mechanisms of terrestrial gamma-ray flashes. *Journal of Geophysical Research*, *113*, D10103. https://doi.org/10.1029/2007JD009248

Dwyer, J. R. (2012). The relativistic feedback discharge model of terrestrial gamma ray flashes. *Journal of Geophysical Research*, *117*, A02308. https://doi.org/10.1029/2011JA017160

Dwyer, J. R., & Cummer, S. A. (2013). Radio emissions from terrestrial gamma-ray flashes. *Journal of Geophysical Research: Space Physics*, *118*, 3769–3790. https://doi.org/10.1002/jgra.50188

Dwyer, J. R., Liu, N., Eric Grove, J., Rassoul, H., & Smith, D. M. (2017). Characterizing the source properties of terrestrial gamma ray flashes. *Journal of Geophysical Research: Space Physics*, *122*, 8915–8932. https://doi.org/10.1002/2017JA024141

Dwyer, J. R., & Smith, D. M. (2005). A comparison between Monte Carlo simulations of runaway breakdown and terrestrial gamma-ray flash observations. *Geophysical Research Letters*, *32*, L22804. https://doi.org/10.1029/2005GL023848

Dwyer, J. R., Smith, D. M., & Cummer, S. A. (2012). High-energy atmospheric physics: Terrestrial gamma-ray flashes and related phenomena. *Space Science Reviews*, *173*(1-4), 133–196. https://doi.org/10.1007/s11214-012-9894-0

Dwyer, J. R., Smith, D. M., Uman, M. A., Saleh, Z., Grefenstette, B., Hazelton, B., & Rassoul, H. K. (2010). Estimation of the fluence of high-energy electron bursts produced by thunderclouds and the resulting radiation doses received in aircraft. *Journal of Geophysical Research*, *115*, D09206. https://doi.org/10.1029/2009JD012039

Dwyer, J. R., & Uman, M. A. (2014). The physics of lightning. *Physics Reports*, *534*(4), 147–241. https://doi.org/10.1016/j.physrep.2013.09.004

Enoto, T., Wada, Y., Furuta, Y., Nakazawa, K., Yuasa, T., Okuda, K., et al. (2017). Photonuclear reactions triggered by lightning discharge. *Nature*, *551*(7681), 481–484. https://doi.org/10.1038/nature24630

Fierro, A. O., Mansell, E. R., Ziegler, C. L., & MacGorman, D. R. (2015). Explicitly simulated electrification and lightning within a tropical cyclone based on the environment of Hurricane Isaac (2012). *Journal of the Atmospheric Sciences*, *72*(11), 4167–4193. https://doi.org/10.1175/JAS-D-14-0374.1

Fishman, G. J., Bhat, P. N., Mallozzi, R., Horack, J. M., Koshut, T., Kouveliotou, C., et al. (1994). Discovery of intense gamma-ray flashes of atmospheric origin. *Science*, *264*(5163), 1313–1316. https://doi.org/10.1126/science.264.5163.1313

Gehrels, N. (1986). Confidence limits for small numbers of events in astrophysical data. *The Astrophysical Journal*, *303*, 336–346. https://doi.org/10.1086/164079

Hare, B. M., Uman, M. A., Dwyer, J. R., Jordan, D. M., Biggerstaff, M. I., Caicedo, J. A., et al. (2016). Ground-level observation of a terrestrial gamma ray flash initiated by a triggered lightning. *Journal of Geophysical Research: Atmospheres*, *121*, 6511–6533. https://doi.org/10.1002/2015JD024426

Knoll, G. F. (2010). *Radiation detection and measurement* (4th ed., xxvi ed.p. 830). Hoboken, NJ: John Wiley.

Lu, G., Blakeslee, R. J., Li, J., Smith, D. M., Shao, X.-M., McCaul, E. W., et al. (2010). Lightning mapping observation of a terrestrial gamma-ray flash. *Geophysical Research Letters*, *37*, L11806. https://doi.org/10.1029/2010GL043494

Lu, G., Cummer, S. A., Li, J., Han, F., Smith, D. M., & Grefenstette, B. W. (2011). Characteristics of broadband lightning emissions associated with terrestrial gamma ray flashes. *Journal of Geophysical Research*, *116*, A03316. https://doi.org/10.1029/2010JA016141

Mailyan, B. G., Briggs, M. S., Cramer, E. S., Fitzpatrick, G., Roberts, O. J., Stanbro, M., et al. (2016). The spectroscopy of individual terrestrial gamma-ray flashes: Constraining the source properties. *Journal of Geophysical Research: Space Physics*, *121*, 11,346–11,363. https://doi.org/10.1002/2016JA022702

Marisaldi, M., Fuschino, F., Labanti, C., Galli, M., Longo, F., Del Monte, E., et al. (2010). Detection of terrestrial gamma ray flashes up to 40 MeV by the AGILE satellite. *Journal of Geophysical Research*, *115*, A00E13. https://doi.org/10.1029/2009JA014502

Price, C., Asfur, M., & Yair, Y. (2009). Maximum hurricane intensity preceded by increase in lightning frequency. *Nature Geoscience*, *2*(5), 329–332. https://doi.org/10.1038/ngeo477

Roberts, O., Chronis, T., Fitzpatrick, G., Bedka, K. M., McBreen, S., Briggs, M. S., et al. (2016). Terrestrial gamma-ray flashes due to particle acceleration in tropical storm systems, AGU Fall Meeting Abstracts, 32.

Rogers, R. F., Aberson, S., Bell, M. M., Cecil, D. J., Doyle, J. D., Kimberlain, T. B., et al. (2015). Re-writing the tropical record books: The extraordinary intensification of Hurricane Patricia. *Bulletin of the American Meteorological Society*. https://doi.org/10.1175/bams-d-16-0039.1

Saunders, C. P. R., & Peck, S. L. (1998). Laboratory studies of the influence of the rime accretion rate on charge transfer during crystal/graupel collisions. *Journal of Geophysical Research*, *103*, 13,949–13,956. https://doi.org/10.1029/97JD02644

Shao, X.-M., Hamlin, T., & Smith, D. M. (2010). A closer examination of terrestrial gamma-ray flash-related lightning processes. *Journal of Geophysical Research*, *115*, A00E30. https://doi.org/10.1029/2009JA014835

Smith, D. M., Buzbee, P., Kelley, N. A., Infanger, A., Holzworth, R. H., & Dwyer, J. R. (2016). The rarity of terrestrial gamma-ray flashes: 2. RHESSI stacking analysis. *Journal of Geophysical Research: Atmospheres*, *121*, 11,382–11,404. https://doi.org/10.1002/2016JD025395

Smith, D. M., Dwyer, J. R., Hazelton, B. J., Grefenstette, B. W., Martinez-McKinney, G. F. M., Zhang, Z. Y., et al. (2011). A terrestrial gamma ray flash observed from an aircraft. *Journal of Geophysical Research*, *116*, D20124. https://doi.org/10.1029/2011JD016252

Smith, D. M., Hazelton, B. J., Grefenstette, B. W., Dwyer, J. R., Holzworth, R. H., & Lay, E. H. (2010). Terrestrial gamma ray flashes correlated to storm phase and tropopause height. *Journal of Geophysical Research*, *115*, A00E49. https://doi.org/10.1029/2009JA014853

Smith, D. M., Lopez, L. I., Lin, R. P., & Barrington-Leigh, C. P. (2005). Terrestrial gamma-ray flashes observed up to 20 MeV. *Science*, *307*(5712), 1085–1088. https://doi.org/10.1126/science.1107466

Splitt, M. E., Lazarus, S. M., Barnes, D., Dwyer, J. R., Rassoul, H. K., Smith, D. M., et al. (2010). Thunderstorm characteristics associated with RHESSI identified terrestrial gamma ray flashes. *Journal of Geophysical Research*, *115*, A00E38. https://doi.org/10.1029/2009JA014622

Stanley, M. A., Shao, X.-M., Smith, D. M., Lopez, L. I., Pongratz, M. B., Harlin, J. D., et al. (2006). A link between terrestrial gamma-ray flashes and intracloud lightning discharges. *Geophysical Research Letters*, *33*, L06803. https://doi.org/10.1029/2005GL025537

Takahashi, T. (1978). Riming electrification as a charge generation mechanism in thunderstorms. *Journal of the Atmospheric Sciences*, *35*(8), 1536–1548. https://doi.org/10.1175/1520-0469(1978)035%3C1536:REAACG%3E2.0.CO;2

Tavani, M., Argan, A., Paccagnella, A., Pesoli, A., Palma, F., Gerardin, S., et al. (2013). Possible effects on avionics induced by terrestrial gamma-ray flashes. *Natural Hazards and Earth System Sciences*, *13*(4), 1127–1133. https://doi.org/10.5194/nhess-13-1127-2013

Tran, M. D., Rakov, V. A., Mallick, S., Dwyer, J. R., Nag, A., & Heckman, S. (2015). A terrestrial gamma-ray flash recorded at the Lightning Observatory in Gainesville, Florida. *Journal of Atmospheric and Solar-Terrestrial Physics*, *136*, 86–93. https://doi.org/10.1016/j.jastp.2015.10.010

Ursi, A., Guidorzi, C., Marisaldi, M., Sarria, D., & Frontera, F. (2017). Terrestrial gamma-ray flashes in the BeppoSAX data archive. *Journal of Atmospheric and Solar-Terrestrial Physics*, *156*, 50–56. https://doi.org/10.1016/j.jastp.2017.02.014

Williams, E., Downes, E., Boldi, R., Lyons, W., & Heckman, S. (2007). Polarity asymmetry of sprite-producing lightning: A paradox? *Radio Science*, *42*, RS2S17. https://doi.org/10.1029/2006RS003488